OXFORD

Social Cognitive and Affective Neuroscience, 2023, **18**(1), 1–12

DOI: https://doi.org/10.1093/scan/nsad018
Advance Access Publication Date: 24 March 2023
Original Manuscript

Distraction and cognitive control independently impact parietal and prefrontal response to pain

Nicolas Silvestrini[1] and Corrado Corradi-Dell'Acqua[2,3]

[1]Geneva Motivation Lab, Faculty of Psychology and Educational Sciences, University of Geneva, Geneva 1205, Switzerland
[2]Theory of Pain Lab, Faculty of Psychology and Educational Sciences, Section of Psychology, University of Geneva, Geneva 1205, Switzerland
[3]Geneva Neuroscience Center, University of Geneva, Geneva, Switzerland
Correspondence should be addressed to Nicolas Silvestrini, Department of Psychology, UNI-MAIL, 40, Boulevard du Pont d'Arve, Geneva CH-1205, Switzerland.
E-mail: nicolas.silvestrini@unige.ch.

Abstract

Previous studies have found that distracting someone through a challenging activity leads to hypoalgesia, an effect mediated by parietal and prefrontal processes. Other studies suggest that challenging activities affect the ability to regulate one's aching experiences, due to the partially common neural substrate between cognitive control and pain at the level of the medial prefrontal cortex. We investigated the effects of distraction and cognitive control on pain by delivering noxious stimulations during or after a Stroop paradigm (requiring high cognitive load) or a neutral condition. We found less-intense and unpleasant subjective pain ratings during (compared to after) task execution. This hypoalgesia was associated with enhanced activity at the level of the dorsolateral prefrontal cortex and the posterior parietal cortex, which also showed negative connectivity with the insula. Furthermore, multivariate pattern analysis revealed that distraction altered the neural response to pain, by making it more similar to that associated with previous Stroop tasks. All these effects were independent of the nature of the task, which, instead, led to a localized neural modulation around the anterior cingulate cortex. Overall, our study underscores the role played by two facets of human executive functions, which exert an independent influence on the neural response to pain.

Keywords: Stroop; attention; connectivity; cingulate; insula

Introduction

Previous studies established that pain engages and interacts with high-level executive functions (Tracey and Mantyh, 2007; Bushnell *et al.*, 2013; Wiech, 2016). For instance, distracting someone through a concurrent activity might reduce one's sensitivity to pain (Petrovic *et al.*, 2000; Tracey *et al.*, 2002; Valet *et al.*, 2004; Buhle and Wager, 2010). At the neural level, distraction hypoalgesia has been associated not only with decreased activity in regions relevant to pain processing, like somatosensory and insular cortices (Petrovic *et al.*, 2000; Valet *et al.*, 2004; Seminowicz and Davis, 2007b), but also with enhanced signal within the prefrontal cortex and periaqueductal grey (Petrovic *et al.*, 2000; Tracey *et al.*, 2002; Valet *et al.*, 2004). These effects have been interpreted consistently with the neurocognitive model of attention to pain according to which bottom-up nociceptive inputs can engage one's attention in competition with top-down processes, such as prefrontal and parietal mechanisms for maintaining attentional load and the processing of goal-relevant stimuli (Legrain *et al.*, 2009).

Despite the overall consensus, several considerations put into question the role played by distraction on pain sensitivity. For instance, some studies failed to replicate the effect (McCaul *et al.*, 1992; Duker *et al.*, 1999) or, at least, limit its efficacy to a subgroup of individuals (Keogh *et al.*, 2000; Seminowicz *et al.*, 2004; Nouwen *et al.*, 2006; Seminowicz and Davis, 2007a). Furthermore, distraction is often manipulated by delivering pain 'During' the execution of highly demanding tasks (e.g. Stroop and N-Back), which, however, exert extensively individual control/regulatory processes by asking to select an appropriate response among multiple competing information. Cognitive control might influence pain experience independently of distraction, as suggested by the studies describing changes in the sensitivity to pain delivered 'After' a Stroop task (Silvestrini and Rainville, 2013; Hoegh *et al.*, 2019; Silvestrini *et al.*, 2020) compared to an easier activity such as counting neutral words. Furthermore, pain and cognitive control disclose distinct but co-localized neural networks (Kragel *et al.*, 2018; Silvestrini *et al.*, 2020), which are integrated at the level of the medial prefrontal cortex (Shackman *et al.*, 2011; Silvestrini *et al.*, 2020), partly reminiscently of the neural structures held to mediate distraction hypoalgesia. In this view, it is unclear whether (and to which extent) the effects of distraction on pain are partly confounded by those of cognitive control.

Received: 30 August 2022; **Revised:** 9 March 2023; **Accepted:** 22 March 2023

Partial evidence in favour of the independence of the two processes arises from the studies modulating parametrically the cognitive load of the distracting task, who failed to find a consequent linear influence on pain sensitivity (Hodes *et al.*, 1990; McCaul *et al.*, 1992; Seminowicz and Davis, 2007b). However, to our knowledge, the effects of distraction and cognitive control on the behavioural and neural response to pain have never been investigated independently.

In this study, we administered noxious thermal stimulations 'During' or 'After' (factor TIMING) an interfering Stroop (with high control load) or an easier paradigm requiring counting neutral words (factor TASK) whilst recording pain-related ratings and neural response through functional magnetic resonance imaging (fMRI). We predicted typical effects of distraction when pain was administered 'During' a task, with associated modulations at the level of prefrontal-parietal structures. Moreover, we tested the effects of cognitive control when comparing the Stroop Interference *vs* the easier condition. The critical question, however, is whether TIMING and TASK influence pain experience independently or whether instead they interact with one another.

Methods

Participants and design

Twenty-nine participants (11 males, mean age = 23.86 ± 4.75 *s.d.*) were recruited by announcement at the University of Geneva. Participants were free of self-reported acute or chronic pain and cardiovascular, neurological or psychological disease. They signed an informed consent prior to the experiment. This research was conducted in accordance with the Declaration of Helsinki and was approved by the local ethical committee.

Painful thermal stimulation

A computer-controlled thermal stimulator with a 25 × 50 mm fluid-cooled Peltier probe (MSA Thermotest, Somedic, Hörby, Sweden) delivered painful thermal stimulations. The baseline temperature was set to 36°C, and each stimulation lasted 16 s (3 s of temperature increase, 10 s of plateau and 3 s of temperature decrease). The temperature of the painful stimulations was adjusted for each participant using a calibration procedure.

fMRI data acquisition

A Siemens Trio 3-T whole-body scanner was used to acquire both T1-weighted anatomical images and gradient-echo planar T2*-weighted images with blood oxygenation level–dependent (BOLD) contrast. Structural images were acquired with a T1-weighted sequence (repetition time = 1900 ms, inversion time = 900 ms, echo time = 2.27 ms and 1 × 1 × 1 mm voxel size). The functional sequence was a trajectory-based reconstruction sequence with a repetition time of 2100 ms, an echo time of 30 ms, a flip angle of 90°, in-plane resolution 64 × 64 voxels (voxel size 3 × 3 mm), 32 slices, a slice thickness of 3 mm and no gap between slices.

Experimental paradigm

Before the scanning session, participants were seated in front of a computer. The probe of the thermal stimulator was installed on their right leg in the lower part of the shinbone, and the individual painful temperature was identified through a staircase procedure (Silvestrini *et al.*, 2020; Silvestrini and Corradi-Dell'Acqua, 2022). We applied three series of ascending and descending thermal stimulations. Participants rated the unpleasantness of each stimulation with a visual analogue scale (VAS) ranging from 0 ('Not unpleasant at all') to 100 ('The most unpleasant pain imaginable'). After an initial increase by steps of 2°C, the temperature started decreasing when participants rated pain unpleasantness as >70 and increased again when pain unpleasantness was <50. The last series of ascending and descending stimulations included steps of 1°C. Based on participants' ratings, we selected a temperature that elicited a pain unpleasantness response of ~70 (temperature: $M = 47.07$, $s.d. = 1.83$ and range = 42–51). The selected temperature remained constant throughout the main experiment.

Then, participants were engaged in a practice session for a Stroop paradigm from previous research (Silvestrini and Rainville, 2013; Silvestrini *et al.*, 2020; Riontino *et al.*, 2022). They were exposed to sets of one-to-four identical words presented vertically on the screen in capital letters (font Verdana and size 24). They were asked to report the number of words displayed (regardless of their meaning) as quickly/accurately as possible. Moreover, participants were asked not to blur their vision preventing them to count effortlessly the words. In the interference condition, the words used were one of 'one', 'two', 'three' and 'four' (in French, 'un', 'deux', 'trois' and 'quatre'), so that it was always inconsistent with the correct response. In the neutral condition, we used instead words of matched length that were not held to elicit any interference: 'year', 'sheet', 'table' and 'skittle' (in French, 'an', 'drap', 'table' and 'quille'). Trials started with a fixation cross (750 ms) followed by the words that stayed on the screen until a response was delivered (but never >1250 ms). Participants then received feedback about their proficiency.

Subsequently, participants were installed on the scanner bed, where they underwent two functional runs of 21 min each, separated by the anatomical scan (see Figure 1 for the design structure). Both scanning runs began with a painful thermal stimulation used as a baseline pain induction. After the stimulation, participants rated subjective pain intensity and unpleasantness by moving with their fingers a cursor displayed on the screen over two VAS, ranging from 'No pain/Not unpleasant at all' (0) to 'The most intense/unpleasant pain imaginable' (100). Then, participants performed four blocks of the Stroop task. However, different from the practice session, the feedback provided was uninformative of one's performance. The feedback appeared for 2 s minus participants' reaction time, ensuring that all trials had the same length (3.4 s). Inter-trial intervals varied randomly (750–1500 ms). In the 'During' condition, the blocks included 36 trials (2 min 30 s), and a thermal stimulation was administered at the 32nd trial, while the participants were performing the remaining four trials. In the 'After' condition, the blocks included 32 trials (2 min), and a stimulation was administered right after the end of the task. Each run included the four possible blocks ('During/Interference', 'After/Interference', 'During/Neutral' and 'After/Neutral'), which were separated by a short break of 12 s. The order of the blocks was counterbalanced within the runs. At the end of the task and stimulation, participants rated pain and unpleasantness associated with the thermal event (total rating time: 24 s) and one item of perceived task difficulty ('How difficult was it for you to achieve the task successfully?'; 'Not at all' [0] to 'Very difficult' [10]).

The experiment was administered using Eprime 2.0 Software (Psychology Software Tools Inc., Pittsburgh, PA, USA). Images were displayed on a computer monitor back projected onto a screen and viewed on a mirror placed on the head coil.

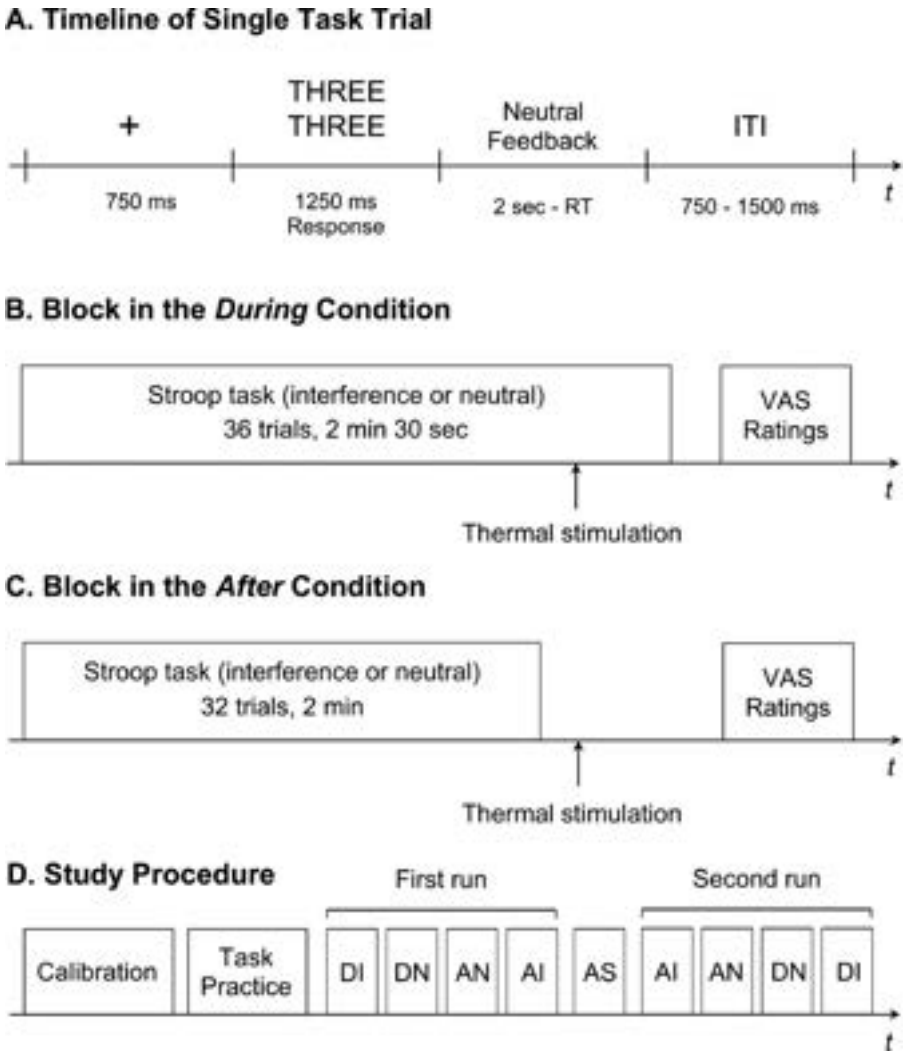

Fig. 1. The timeline of a single-task trial (A), an overview of experimental blocks in the During (B) and the After (C) conditions and an overview of the study protocol (D). Neutral feedback: 'Response recorded' or 'Please answer more quickly' in case of no response. ITI: inter-trial interval, AS: anatomical scan, DI: During-Interference, DN: During-Neutral, AN: After-Neutral, AI: After-Interference. The order of the experimental conditions was counterbalanced across subjects.

Data processing

Behavioural data

For each subject and condition, the average Accuracy and median correct Reaction Times from Stroop trials were analysed with a paired-sample *t*-test probing differences between Interference *vs* Neutral TASK conditions. As for participants' ratings, the average Intensity and Unpleasantness values were analysed with repeated-measures ANOVA, with TIMING (During *vs* After) and TASK (Interference *vs* Neutral) as within-subject factors. The analysis was run using R 4.0.4 software (http://cran.r-project.org).

Imaging processing

Preprocessing. Statistical analysis was performed using the SPM12 software (http://www.fil.ion.ucl.ac.uk/spm/), exploiting the preprocessing pipeline from the CONN 21 toolbox (https://web.conn-toolbox.org/, Whitfield-Gabrieli and Nieto-Castanon, 2012). For each subject, functional images were realigned, unwrapped and slice-time corrected. The Artifact Detection Tools, embedded in the CONN toolbox, were then used for the identification of outlier scans in terms of excessive subject motion and signal intensity spikes. Finally, the images were then normalized to a template based on 152 brains from the Montreal Neurological Institute with a voxel-size resolution of 2 × 2 × 2 mm and smoothed by convolution with an 8 mm full width at half-maximum Gaussian kernel.

First-level analysis. Preprocessed images from each task were analysed using the General Linear Model (GLM) framework implemented in SPM. Our key event of interest was pain trials. Hence, for each functional run, we modelled the onset of each thermal stimulation with a boxcar function of 10 s duration starting the moment in which the thermode reached the plateau temperature. Thermal events were specified separately according to the associated experimental condition ('During/Interference', 'After/Interference', 'During/Neutral' and 'After/Neutral'). Additionally, the baseline stimulation, conducted at the beginning of each functional run, was modelled as a separate vector. In addition to the main analysis, we also looked at the neural responses evoked by the Stroop task, where each of the two conditions ('Interference' and 'Neutral') was delivered through

~2 min blocks. Although optimal for testing cognitive control after-effects on pain (Silvestrini and Rainville, 2013; Silvestrini *et al.*, 2020; Riontino *et al.*, 2022), such a long block structure would make the analysis of task-related activity vulnerable to low-frequency confounds and poorly accords with default filtering in SPM (128 s). To circumvent this, we analysed specific Stroop trials in an event-related fashion as a delta function (without distinguishing between 'Interference' and 'Neutral' condition) and specifying an additional predictor in which trials' Reaction Times were modulated parametrically. This parametric predictor was our measure of interest for Stroop-related activity, as it should capture both differences between 'Interference' and 'Neutral' conditions ('Interference' trials take on average longer, see Results) but also inter-trial fluctuations in performance and, as such, should be less vulnerable to signal low-frequency noise/drifts. Supplementary Information provides additional analyses on an independent dataset (Verstynen, 2014), showing that such an approach represents a reliable test for neural responses of Stroop demands. Overall, we specified seven predictors for each functional run (four main thermal stimulations, one baseline thermal stimulation, one Stroop and one Reaction Times parametrical modulation), which were convolved with a canonical hemodynamic response function and associated with their first-order temporal derivative. To account for movement-related variance, and other sources of noise, we included the six differential movement parameters from the realignment (x, y and z translations and pitch, roll and yaw rotations) and dummy variables' signalling outlier scans (from the ART toolbox) as covariates of no interest. Low-frequency signal drifts were filtered using a cut-off period of 128 s, and serial correlation in the neural signal was accounted through the first-order autoregressive model AR(1).

Second-level analyses. Functional contrasts, testing differential parameter estimate images associated with one experimental condition *vs* the other, were then analysed through a second-level one-sample *t*-test using random-effects analysis. The effects were identified as significant only if they exceeded a family-wise error cluster-level correction for multiple comparisons at the whole brain (Friston *et al.*, 1993), with an underlying voxel-level threshold corresponding to $P < 0.001$ (uncorrected).

Functional connectivity. Preprocessed images were denoised through the default pipeline in CONN toolbox to remove components in the neural signal which were related to (1) white matter and cerebro-spinal fluid signal (first 15 principal components), (2) estimated subject movement parameters (from preprocessing), (3) the presence of outlier scans (estimated through the ART toolbox during preprocessing), and (4) task-related BOLD signals (in our case, pain-evoked activity and stroop trials). Data was also band-pass filtered (0.008-0.09 Hz) to account both for slow-frequency fluctuations and well as physiological and residual movement artefacts. Subsequently, denoised data was analyzed through ROI-to-ROI connectivity using generalized psychophysiological interaction (gPPI) (McLaren *et al.*, 2012). For this analysis we considered the ROIs from Brainnetome parcellation of the human brain (Fan *et al.*, 2016). This allows for a whole-brain fine-grain exploration of the regions involved without any a priori assumption on the implicated network. In particular, we focused on 224 ROIs comprehending the whole atlas, except for the regions 189-210 corresponding to the occipital cortex (Fan et al., 2016, Table 1) which were outside our range of interest. gPPI is a task-dependent connectivity analysis computing how strongly the BOLD response time course of two regions are coupled in a given condition (in our case, thermal stimulations). This is implemented though a regression model, whereby the time course of target ROIs is regressed against that of a seed ROI multiplied with the psychological variable. Within the network of interest, every possible combination of seed-target ROIs was considered, thus leading to a 224 x 224 regression coefficients (βs) matrix for each participant and condition. For group-level analysis, individual βs were converted to z-scores with Fisher's transformation. Functional contrasts, testing coupling parameters associated with one experimental condition vs. the other were then fed in a second level random-effect analysis. To identify conditions of interest, we applied Spatial Pairwise Clustering correction (Zalesky *et al.*, 2012), as implemented in the CONN 21 toolbox. This approach is reminiscent to the cluster-based correction for multiple comparisons for fMRI activation: in this case regression coefficients are clustered together based on hierarchical cluster analysis based on both functional and spatial criteria (weighting factor 0.5). The cluster mass of connections exceeding a height threshold corresponding to $p < 0.01$ (uncorrected) was validated statistically based on the null distribution of obtained through 1000 permutations of the original dataset. In particular, clusters were identified as significant if exceeding False Discovery Rate (FDR) correction at $P < 0.05$.

Table 1. Stroop task: parametric modulation of Reaction Times. The implicated regions survive FWE correction for multiple comparisons at the cluster level, with an underlying voxel-level threshold corresponding to $P < 0.001$. L and R refer to the left and right hemispheres, respectively. M refers to medial activations

		Coordinates				
	Side	x	y	z	$t_{(28)}$	Cluster size
Parametric modulation of Response Times						
Middle cingulate gyrus	M	−10	20	30	7.63	73 685***
Supplementary motor area	M	−4	8	50	8.78	
Precuneus	M	−10	−66	54	9.04	
PPC	L	−38	−32	50	9.55	
PPC	R	44	−36	42	8.71	
AI	L	−28	22	2	10.04	
Inferior frontal gyrus	L	−50	12	2	6.75	
Caudate	L	−10	4	10	7.66	
Thalamus	L	−10	−18	8	8.27	
AI	R	30	26	0	8.49	
Inferior frontal gyrus	R	52	12	2	6.07	
Caudate	R	10	6	6	6.68	
Thalamus	R	10	−10	6	9.71	
DLPFC	R	40	36	18	7.18	
Inferior temporal gyrus	L	−52	−62	−8	7.85	
Inferior temporal gyrus	R	56	−52	−10	7.24	
Inferior occipital gyrus	L	−32	−86	0	6.22	
Inferior occipital gyrus	R	36	−88	−2	6.28	
Midbrain	M	8	−22	−12	5.78	
Cerebellum	L	−24	−70	−48	7.65	
Cerebellum	R	22	−48	−26	12.26	

***$P < 0.001$; corrected for multiple comparisons at the cluster level for the whole brain.

Multivariate pattern analysis. We used multivariate models predictive of subjective pain (Sharvit *et al.*, 2020) and Stroop demands (Silvestrini *et al.*, 2020) from neural activity to assess whether brain-based estimates of pain unpleasantness and Stroop effect, respectively, changed as a function of the manipulated conditions. The pain model is a radial-basis function kernel Support Vector Regression trained on principal components of brain activity evoked by thermal stimulations at three levels of unpleasantness from previous data. The model was subsequently validated both within the sample used for the estimation (through leave-one-out cross-validation) and on an independent cohort (see Sharvit *et al.*, 2020). The Stroop model is a linear Support Vector Classification discriminating between Stroop Interference *vs* Neutral conditions on a previous dataset (Silvestrini *et al.*, 2020). Also, this model was validated within the sample used for the estimation. Furthermore, we now report in the Supplementary Information an independent validation of the dataset from Verstynen (2014), revealing how the original model was able to efficiently detect high Stroop demands both in terms of task-preordained conditions (Interference *vs* Neutral) and when modeling trials as a function of participants' Response Times though an *ad hoc* GLM where trials with longest responses in each session were specified separately from those with the most rapid reactions (through median split).

We obtained brain-based estimations of Pain Unpleasantness and Stroop demands for each participant and condition by calculating the dot product between the model parameters and first-level brain activity. The resulting values were then analysed at the group level through the same ANOVA and *t*-test approaches used for the behavioural measures. Full details on how the models were developed and validated (including links to codes for their generalization to new data) are available in the Supplementary Information.

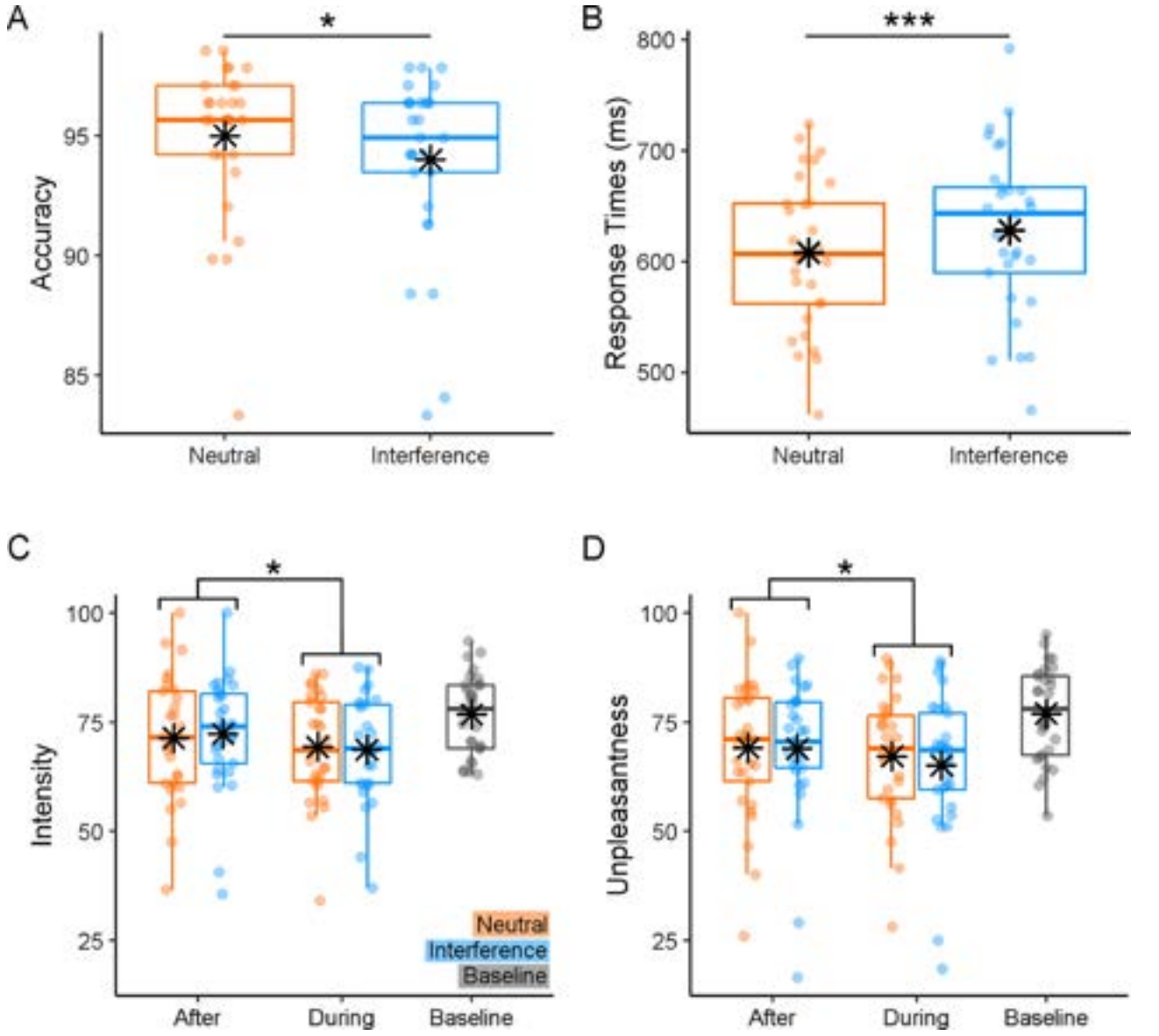

Fig. 2. The behavioural responses. Boxplots and individual data describing (A, B) average Accuracy and median correct Reaction Times associated with the Stroop Task and (C, D) average Pain Intensity and Unpleasantness ratings associated with the thermal stimulations. For each boxplot, the horizontal line represents the median value of the distribution, the star represents the average, the box edges refer to the interquartile range and the whiskers refer to the data range within 1.5 of the interquartile range. Individual data points are also displayed as dots. '***' and '*' refer to significant condition differences at $P < 0.001$ and $P < 0.05$, respectively.

Results

Behavioural responses

Stroop performance

We confirmed that participants were both less accurate (95% *vs* 94%, $t_{(28)} = -2.39$, $P = 0.024$, Cohen's $d = -0.44$) and slower at responding correctly (607.98 *vs* 628.03 ms, $t_{(28)} = 4.47$, $P < 0.001$, $d = 0.83$) during the Interference, as opposed to the Neutral condition (see Figure 2A, B). Additionally, follow-up analyses revealed that task performance was negatively impacted by the onset of the thermal stimulation (see Supplementary Results for more details).

Thermal ratings

We analysed thermal ratings through an ANOVA, which revealed a main effect of TIMING (Pain Intensity: $F_{(1,28)} = 7.88$, $P = 0.014$, $\eta_p^2 = 0.22$; Unpleasantness: $F_{(1,28)} = 6.25$, $P = 0.018$, $\eta_p^2 = 0.19$). Individuals felt painful temperatures as less intense (69.02 *vs* 71.84) and unpleasant (66.17 *vs* 69.01) 'During' the task rather 'After' its completion (see Figure 2C, D). No significant modulation of TASK was found, neither as a main effect nor in interaction with TIMING ($F_{(1,28)} \leq 1.40$, $P \geq 0.246$). Overall, our data confirm previous evidence of distraction hypoalgesia, whereby individuals consider pain less intense and unpleasant while actively engaged in a task.

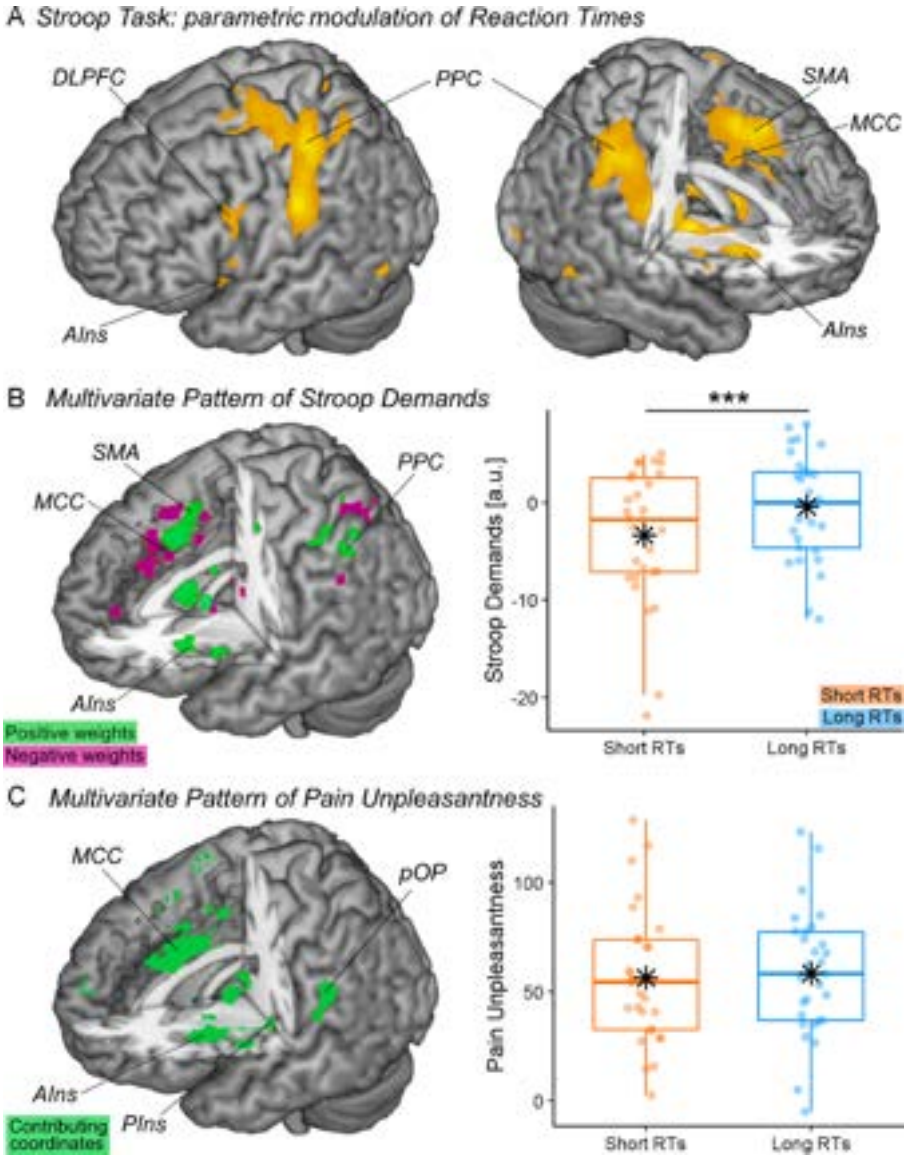

Fig. 3. The stroop activity. (A) The surface rendering showing regions whose activity during the Stroop task increased linearly with the Reaction Times. To improve the readability of this specific plot, regions are displayed at voxel-level FWE correction for multiple comparisons for the whole brain, thus highlighting only brain portions showing the strongest association. (B, C) Predictions from whole-brain models of Stroop demands (Silvestrini *et al.*, 2020) and pain unpleasantness (Sharvit *et al.*, 2020). Each model is described in terms of whole-brain maps with coordinates highlighted based on their relative importance. For the Stroop model, coordinates describe the relative linear positive or negative contribution to the prediction. For pain unpleasantness, coordinates are coded exclusively in terms of non-linear contribution (Sharvit *et al.*, 2020). The output of each model is depicted separately for Stroop trials with long *vs* short response times, as displayed through dedicated boxplots. Vertical values associated with Stroop Demands (in arbitrary units) reflect the degree of similarity between our data and the pattern expressed by the model (see Methods). Vertical values associated with Pain unpleasantness are coded in an unpleasantness scale ranging from 0 to 100. PIns: posterior insula; SMA: supplementary motor area; MCC: middle cingulate cortex; pOP: parietal operculum; a.u.: arbitrary units. '***' refers to significant condition differences at $P < 0.001$.

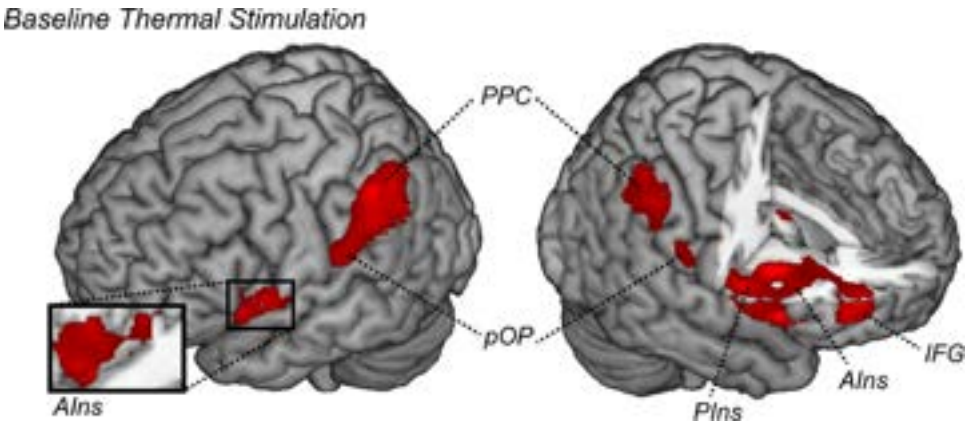

Fig. 4. The baseline temperature. The surface rendering showing regions associated with the delivery of the baseline thermal event (when contrasted with the non-specified parts of the model [implicit baseline]). All regions displayed survive cluster-level FWE correction for multiple comparisons for the whole brain. PIns: posterior insula; pOP: parietal operculum; IFG: inferior frontal gyrus.

Table 2. Thermal stimulations. Regions associated with the delivery of the baseline thermal event (when contrasted with the non-specified parts of the model [implicit baseline]) and with the main effect of TIMING (During > After). All regions survive FWE correction for multiple comparisons at the cluster level, with an underlying voxel-level threshold corresponding to $P < 0.001$

		Coordinates				
	Side	x	y	z	$t_{(28)}$	Cluster size
Baseline Thermal Stimulation						
Posterior insula	L	−30	−18	12	5.75	2175***
Anterior insula	L	−30	6	12	6.97	
Posterior insula	R	42	−4	0	5.90	4408***
Anterior insula	R	38	18	−6	8.20	
Inferior frontal gyrus	R	44	46	2	6.24	
Pallidum	R	18	4	−4	4.47	
Caudate	R	16	16	12	4.31	
PPC	L	−58	−42	48	7.03	547**
Parietal operculum	L	−64	−26	22	4.95	
PPC	R	62	−36	46	5.89	595**
Parietal operculum	R	56	−26	24	5.27	
TIMING main effect: During > After						
DLPFC	L	−36	18	46	6.84	1466***
DLPFC	R	40	22	32	5.24	527**
Dorsomedial prefrontal cortex	M	−2	44	30	4.30	345*
PPC	L	−60	−50	36	4.24	1837***
Superior temporal gyrus	L	−46	−48	20	5.97	
Middle temporal gyrus (post. part)	L	−58	−38	−4	7.62	
Superior temporal gyrus	R	62	−50	14	5.23	700**
Middle temporal gyrus (post. part)	L	54	−28	−6	5.14	
Middle temporal gyrus (ant. part)	R	52	−4	−22	6.02	
Inferior occipital gyrus	L	−24	−98	0	14.47	1640***
Inferior temporal gyrus	L	−44	−56	−14	5.33	
Cerebellum	L	−20	−84	−32	5.51	
Inferior occipital gyrus	R	26	−96	0	9.51	501**

***$P < 0.001$; **$P < 0.01$; *$P < 0.05$ corrected for multiple comparisons at the cluster level for the whole brain.

Neural responses

Stroop performance

We ran a linear regression searching for regions whose activity increased monotonically with the Reaction Times. Consistent with previous studies employing Stroop (Laird *et al.*, 2005; Hung *et al.*, 2018) and other tasks involving cognitive control (Shackman *et al.*, 2011; Hung *et al.*, 2018; Kragel *et al.*, 2018), we implicated a wide network involving the middle cingulate cortex, supplementary motor area, precuneus, anterior insula (AIns), dorsolateral prefrontal cortex (DLPFC), posterior parietal cortex (PPC), thalamus, etc. (Table 1 and Figure 3A). To gather a more stringent functional interpretability of this network, we took a model-based approach and analysed our data through the lens of a multivariate predictive model of Stroop high (*vs* low) demand developed on an independent dataset (Silvestrini *et al.*, 2020; see also Supplementary Information). We confirmed that this model led to a much stronger output for Stroop trials with longer Reaction Times than those processed rapidly ($t_{(28)} = 5.07$, $P < 0.001$, $d = 0.94$; see Figure 3B). Instead, when feeding the same data to whole-brain models predictive of pain unpleasantness (Sharvit *et al.*, 2020), we found no differential output between long *vs* short Reaction Times in Stroop ($t_{(28)} = 0.69$, $P = 0.497$, $d = 0.13$; see Figure 3C). Overall, the activity patterns evoked by Stroop demands appear to be similar to that of previous tasks testing cognitive control via Stroop (Silvestrini *et al.*, 2020), while at the same time they differ from those implicated in thermal pain (Sharvit *et al.*, 2020).

Baseline pain

Subsequently, we inspected the neural responses associated with the delivery of painful temperatures. Figure 4 and Table 2

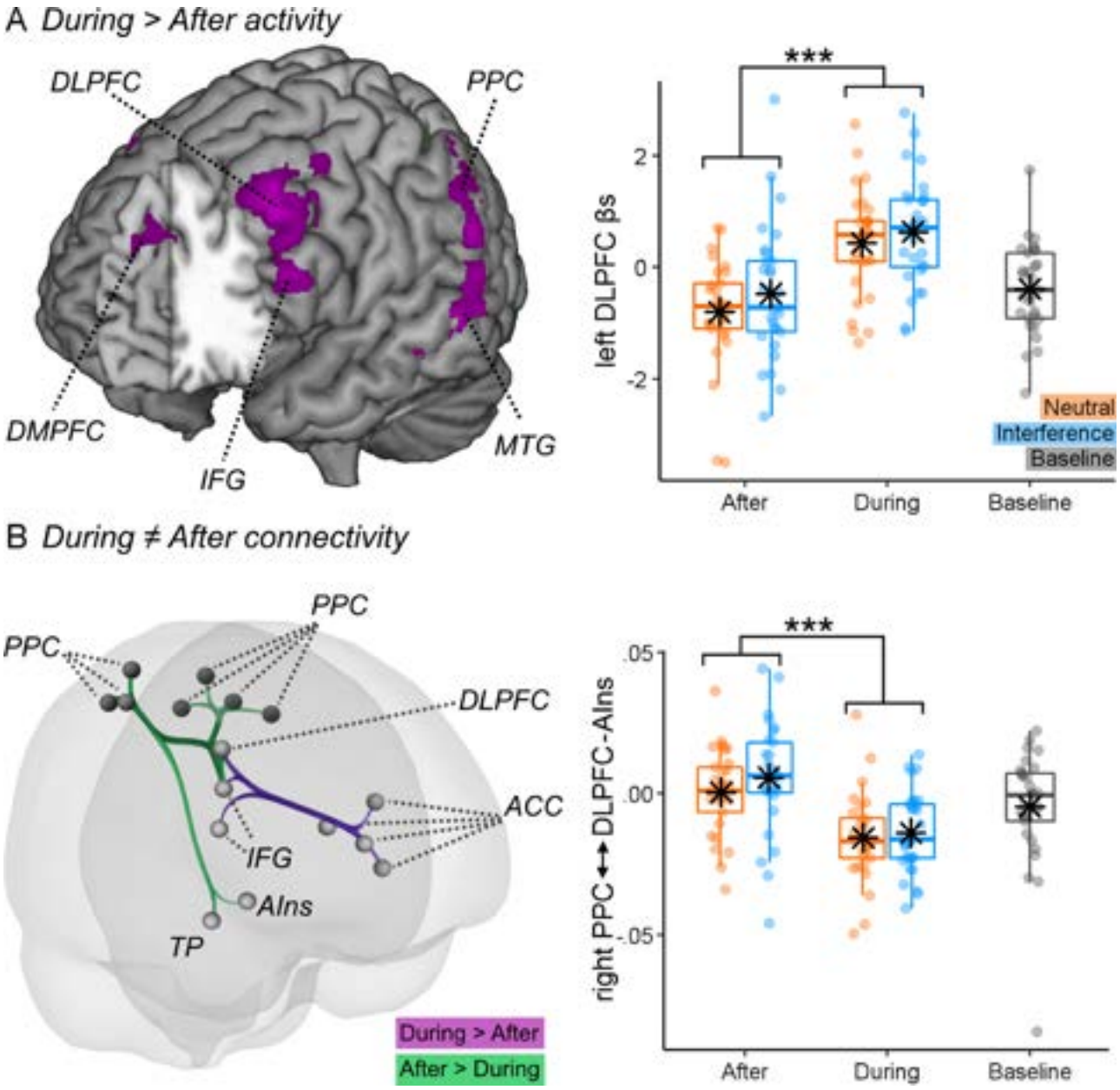

Fig. 5. The distraction-related activity. (A) The surface rendering showing regions associated with the delivery of thermal stimulation 'During' > 'After' the Stroop task. All regions displayed survive FWE correction for multiple comparisons for the whole brain at $P < 0.05$. The parameter estimates from one outlined region of interest are displayed through boxplots and individual data points. (B) The connectivity changes evoked by the delivery of thermal stimulations 'During' *vs* 'After' the task. The connectivity parameters from the track connecting the right parietal cortex to the lateral prefrontal cortex and AI (Cluster 1) are also displayed through boxplots and individual data points. '***' refers to a significant main effect of TIMING at $P < 0.001$. DMPFC: dorsomedial prefrontal cortex; IFG: inferior frontal gyrus; MTG: middle temporal gyrus; ACC: anterior cingulate cortex; TP: temporal pole.

report brain-evoked activity associated with the baseline stimulation introducing each experimental session (relative to the non-specified parts of the model [implicit baseline]) and confirm a widespread network involving bilateral operculum, insula (in both posterior and anterior portions), PPC and right inferior frontal gyrus.

Stroop-related pain

Effects of distraction. We then tested the degree to which pain-evoked activity was influenced by the Stroop task. When analyzing the main effect of TIMING, we found stronger activity 'During' (*vs* 'After') the Stroop task in the bilateral DLPFC, bilateral PPC and middle temporal gyrus. The further activity was observed at the level of the dorsomedial prefrontal cortex (Figure 5A and Table 2). No region displayed stronger activity in the 'After' (*vs* 'During') condition. We analyzed the effect of TIMING also from a connectivity point of view (Table 3). This analysis identified three clusters of connections similarly impacted by the presence of the Stroop task. In particular, the right and left PPC exhibited decreased connectivity with right DLPFC and AI (Figure 5B, green tracks). Additionally, the right DLPFC showed increased connectivity with the cingulate cortex, in both its dorsal anterior cingulate cortex (dACC) and subgenual aspects (Figure 5B,

Table 3. ROI-to-ROI connectivity analysis. Change in functional connectivity associated with the main effect of TIMING. The implicated tracks survive Spatial Pairwise Clustering for multiple comparisons (Zalesky *et al.*, 2012). Each cluster is described in terms of contributing paths, t-test statistic and global Mass index. The name of each region is drawn from the Brainnetome atlas (Fan *et al.*, 2016, Table 1)

Connection	$t_{(28)}$	Mass
R IFJ → R SPL A7r	−4.78***	184.31
R SPL A7c → R STG A38l	−4.65***	
R SPL A7r → R IFG A44d	−4.40***	
R SPL A7r → R IFJ	−3.83***	
R IFG A44d → R SPL A5l	−3.58***	
R SPL A5l → R IFG A44d	−3.56**	
R STG A38l → R SPL A7c	−3.54**	
R SPL A7c → R IFG A44d	−3.49**	
R SPL A7r → R STG A38l	−3.39**	
R IFG A44d → R SPL A7r	−3.39**	
R SPL A7r → R vAI	−3.01**	
R SPL A7c → R IFJ	−2.80**	
R IFG A44d → R SPL A7c	−2.80**	
R IFJ → R SPL A7c	−2.80**	
L SPL A7r → R IFG A44d	−5.05***	154.59
R IFG A44d → L SPL A7r	−3.74***	
L SPL A7r → R IFJ	−3.56**	
L SPL A5l → R IFJ	−3.41**	
R IFG A44d → L SPL A5l	−3.35**	
R IFG A44d → L SPL A7ip	−3.30**	
L SPL A5l → R IFG A44d	−3.31**	
L SPL A7ip → R IFG A44d	−3.27**	
L SPL A7c → R IFJ	−3.21**	
L SPL A7c → R IFG A44d	−3.18**	
R IFJ → R IFG A44d	−3.10**	
R IFJ → L SPL A7c	−2.93**	
R IFG A44d → L SPL A7c	−2.27**	
R IFG A44d → L ACC A32p	4.07***	147.84
L ACC A32p → R IFG A44d	3.98***	
R IFJ → L ACC A32sg	3.88***	
L ACC A32p → R IFJ	3.86***	
R IFG A44d → L ACC A32sg	3.45**	
R IFJ → L ACC A32p	3.43**	
R IFJ → R ACC A24rv	3.30**	
R IFJ → R ACC A32sg	3.30**	
R IFG A45c → L ACC A32p	3.26**	
L ACC A32p → R IFG A45c	3.25**	
R IFG A45c → L ACC A32sg	3.19**	
R ACC A32sg → R IFJ	2.98**	

*** and ** refer to significant modulations at $P < 0.001$ and $P < 0.01$, respectively.

purple tracks). Please note that, although in the During condition pain stimulations and Stroop trials co-occurred, Stroop effects were independently modelled in the first-level analysis by a dedicated predictor. Hence, pain and task effects on the neural signal were not confounded in our results. Indeed, all effects presented here can be interpreted exclusively in terms of pain processing, and how they are influenced by the ongoing task.

Effects of stroop demands. Subsequently, we analyzed the effect played by TASK in pain-evoked activity, both as a main effect and in interaction with TIMING. When applying correction for multiple comparisons for the whole brain no effects were observed. However, under a less conservative threshold (corresponding to $p < 0.001$ uncorrected), we found the dACC implicated in the main effect of TASK (x = 12, y = 38, z = 20, $t_{(28)} = 4.50$ and 122 consecutive voxels), with stronger activity when the pain was associated to the Interference *vs* Neutral condition (Figure 6). No effect was associated with the TASK*TIMING interaction. Finally, no effects of TASK and TASK*TIMING were found at the level of connectivity.

Multivariate patterns To achieve a more reliable functional interpretation of our results, we applied to our pain-evoked responses whole-brain model predictive of pain unpleasantness (Sharvit *et al.*, 2020) and Stroop demands (Silvestrini *et al.*, 2020). More specifically, we analyzed the models' output through the same ANOVA scheme used for subjective ratings. For both models, we found a main effect of TIMING (Pain Unpleasantness: $F_{(1,28)} = 8.74$, $P = 0.006$, $\eta_p^2 = 0.24$; Stroop Demands: $F_{(1,28)} = 5.53$, $P = 0.026$, $\eta_p^2 = 0.17$). Figure 7 displays the models' output across the different conditions and reveals that, consistently with what found for subjective responses, brain estimates of Pain Unpleasantness decreased 'During' *vs* 'After' the task. Instead, brain estimates of Stroop demands during pain showed an opposite trend, as they increased when participants were engaged in the task, rather than subsequent to it. No significant effects were associated with the factor TASK, neither as a main effect nor in interaction with TIMING ($F_{(1,28)} \leq 1.17$, $P \geq 0.289$). Finally, the effects associated with the *Pain Unpleasantness* model could be observed also when adopting a different multivariate predictive model, such as the neurological pain signature from Wager *et al.* (2013). Please see Supplementary Information for full details.

Discussion

We found a dissociation in the role played by distraction and cognitive control in the pain experience. Participants rated the pain as less intense and unpleasant while they were engaged in an active task, consistent with previous research on distraction hypoalgesia (Petrovic *et al.*, 2000; Tracey *et al.*, 2002; Valet *et al.*, 2004; Buhle and Wager, 2010). Such an effect was associated with an increased activity at the level of prefrontal, parietal and temporal structures but also by negative connectivity between PPC and DLPFC–AIns. Finally, multivariate pattern analysis revealed that distraction altered the neural pain response, by making it less similar to that usually observed during thermal stimulations (Sharvit *et al.*, 2020) and more aligned to that associated with Stroop (Silvestrini *et al.*, 2020). Critically, all these effects were observed independently of cognitive control demands of the TASK employed which, instead, led to a selective increase in neural activity around dACC.

Distraction and pain response

Our findings nicely dovetail the predictions from the neurocognitive model of attention to pain (Legrain *et al.*, 2009), which speculates that PPC is associated with individual attentional set, including maintaining the focus on goal-relevant stimuli while inhibiting information from competing sources of information. Consistently, we found increased PPC activity 'During' task execution (Figure 5A) and its negative coupling with AI (Figure 5B). This possibly reflects an inhibitory mechanism that, in turn, can explain previous evidence of decreased insular activity associated with distraction hypoalgesia (Petrovic *et al.*, 2000; Valet *et al.*, 2004; Seminowicz and Davis, 2007b). In this view, multiple studies showed how AI plays a key role in pain appraisal, by integrating bottom-up nociceptive signals with top-down factors related to attention and expectation (Atlas *et al.*, 2010; Geuter *et al.*, 2017; Sharvit *et al.*, 2018). It is therefore likely that the PPC-AI inhibition observed here might nullify these top-down influences, by making one's sensitivity more dependent on incoming ascending inputs.

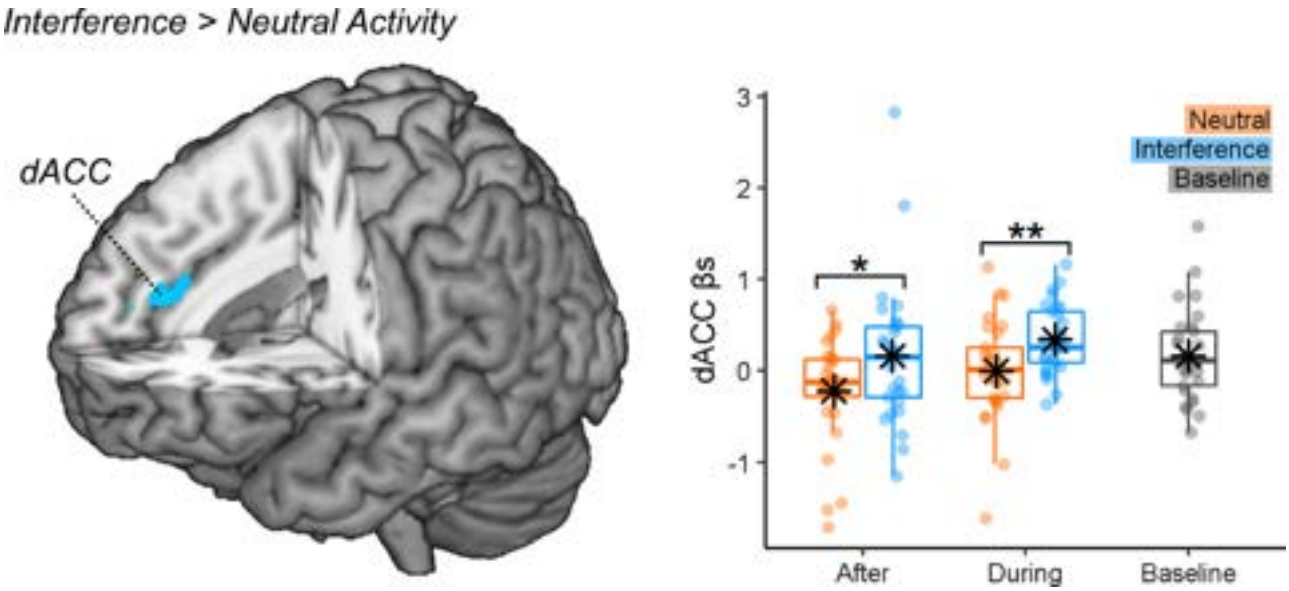

Fig. 6. The task-demands effects on pain activity. The surface rendering showing regions associated with the delivery of thermal stimulations associated with the 'Interference' > 'Neutral' Stroop conditions. The activations are displayed under a threshold corresponding to $P < 0.001$ (uncorrected). The parameter estimates from the outlined region are displayed through boxplots and individual data points. '**' and '*' refer to a significant condition differences at $P < 0.01$ and $P < 0.05$, respectively.

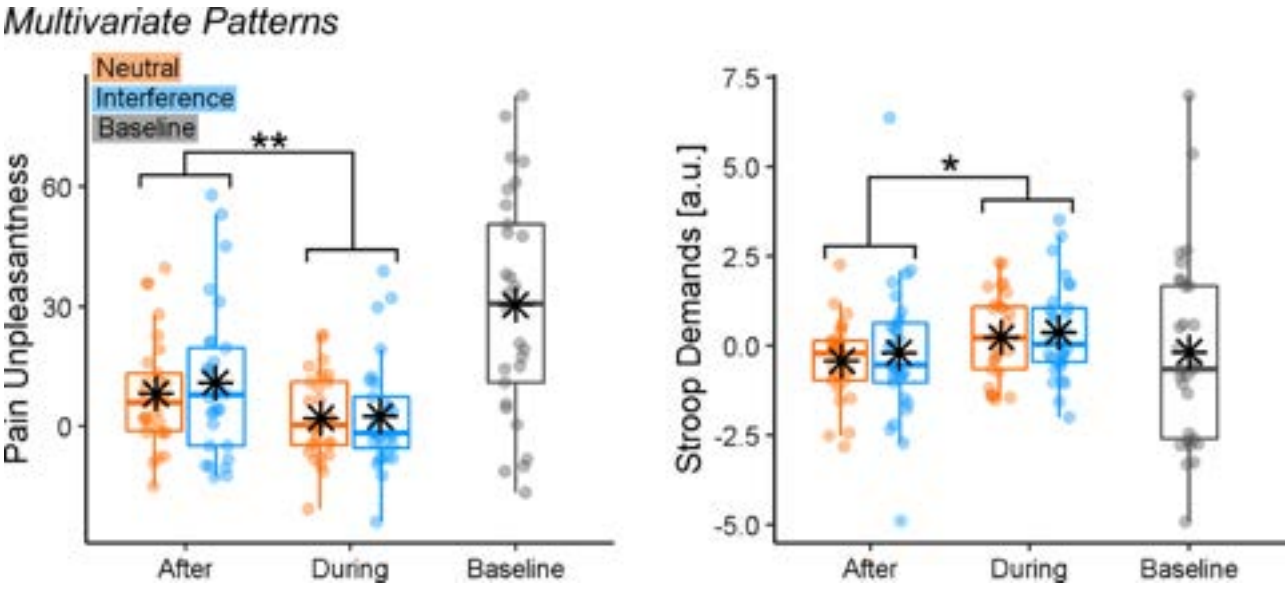

Fig. 7. The multivariate pattern analysis of Stroop-related pain activity. The boxplots and individual data describing the predictions from whole-brain models of Stroop demands (Silvestrini *et al.*, 2020) and pain unpleasantness (Sharvit *et al.*, 2020) applied to the Stroop-related pain activity from our data. '**' and '*'refer to a significant main effect of TIMING from a repeated-measures ANOVA at $P < 0.01$ and $P < 0.05$, respectively.

In line with previous research, we also found that distraction increased the activity at the level of the lateral and medial prefrontal cortex (Petrovic *et al.*, 2000; Valet *et al.*, 2004). However, connectivity analysis suggests that DLPFC activity is highly coupled with that of AI but negatively associated with PPC. It is possible that, differently from PPC, DLPFC underlies compensatory processes that are engaged whenever the signal in structures like AI is high. This interpretation fits the neurocognitive model of attention to pain, which speculates that DLPFC is implicated in maintaining attentional load towards the main task (Legrain *et al.*, 2009), a process that could be recruited to a larger extent when the more competing pain signals are strong.

As for the medial portions of the prefrontal cortex, this region could play a key role in triggering descending regulatory mechanisms for pain at the level of striatum, periaqueductal grey and spinal cord (Valet *et al.*, 2004; Sprenger *et al.*, 2015; Woo *et al.*, 2015; Tinnermann *et al.*, 2017). These pathways have been partly observed in previous research on distraction (Petrovic *et al.*, 2000; Tracey *et al.*, 2002; Valet *et al.*, 2004), thus associating hypoalgesia with a well-known neurobiological model of pain regulation. In principle, the same processes could be at play also in our research although we found no evidence that the medial prefrontal cortex was interacting with the midbrain during distraction.

Cognitive control and pain response

When analysing the effects of TASK, we found enhanced pain responses in dACC associated with an interfering Stroop (*vs* neutral control), regardless of whether this condition preceded or was concurrent with the pain stimulation (Figure 6). These results fit previous findings that identify dACC as a key hub for the interplay between cognitive control and pain (Shackman *et al.*, 2011; Silvestrini *et al.*, 2020). Importantly, although the effects of cognitive control are orthogonal to those associated with distraction, they might not be independent from them as dACC exhibits also enhanced connectivity with DLPFC-AI during task execution. Hence, pain responses in dACC are also influenced by the attentional manipulation, possibly reflecting some degree of overlap between these two facets of human executive functions.

Behaviourally we found no effect of Stroop-induced cognitive control on participants' pain sensitivity. This might appear at odds with the literature that found significant modulations, albeit with different directions (Silvestrini and Rainville, 2013; Hoegh *et al.*, 2019; Silvestrini *et al.*, 2020). It is reasonable that hidden moderators/confounds might have influenced previous and current results. For instance, we recently found that cognitive control after-effects in pain are influenced by the intensity of the noxious input, with mild stimulations associated with hyperalgesia but more intense events with hypoalgesia (Riontino *et al.*, 2022). Hence, it is possible that the stimulation adopted here fell within a 'medium' range where its susceptibility to cognitive control manipulations was minimum. Future studies will need to further investigate the effect of cognitive control and pain sensitivity.

Limitations of the study and conclusive remarks

Given the nature of the research question, our experimental design was constrained by long-task sessions (Silvestrini and Rainville, 2013; Silvestrini *et al.*, 2020), each associated with one thermal stimulation. This made the task-related signal susceptible to low-frequency fluctuations (which was accounted for in the analysis), whereas pain-related activity was based on limited repetitions and with no room for a control painless stimulation. Finally, Figure 2C,D shows a strong desensitization between the first (baseline) thermal stimulation and the subsequent ones. We believe that these limitations have little impact on the main conclusions of the study, which proved to be sufficiently sensitive to capture strong thermal-related increases in the neural signal and associated attentional effects. Furthermore, the neural modulations associated with TIME mirrored closely behavioural measures of pain and unpleasantness. As for the TASK manipulation, the lack of positive behavioural effects might reflect its poor effectiveness at influencing pain response although the same design was effectively used before to document the positive influences of Stroop on pain (Silvestrini and Rainville, 2013; Silvestrini *et al.*, 2020) and vice versa (Silvestrini and Corradi-Dell'Acqua, 2022).

Finally, we acknowledge the difficulty of pulling apart entirely the effects of endogenous attention and cognitive control on pain, as these two processes are highly interconnected and exert mutual influence. A more efficient way for future research could be modulating attention exogenously. However, according to the neurocognitive model of attention (Posner and Petersen, 1990), we may distinguish between executive (cognitive) control, related to conflict monitoring in tasks like the Stroop, and two other cognitive functions, namely alertness and orientation. Accordingly, one might explain distraction associated with the neutral condition in the present study as related to increased alertness independently from cognitive control. Alternatively, one might also consider that counting neutral words requires working memory, due to the maintenance of task goals' representations, which could lead to distraction hypoalgesia (Legrain *et al.*, 2009) and be associated with some degree of cognitive control. Future studies might help to further disentangle this issue.

Keeping these limitations aside, in this study, we investigated the role of distraction and cognitive control in pain, with the former affecting subjective experience and triggering a widespread network involving PPC and DLPFC in interaction with AI and the latter instead affecting specifically dACC. Overall, our study underscores for the first time the independent, and yet concurrent, role played by two different facets of human executive functions in the neural response to pain.

Supplementary data

Supplementary data are available at *SCAN* online.

Funding

N.S. was supported by a Swiss National Science Foundation grant (Grant number PZ00P1_142458). C.C.-D. was supported by Swiss National Science Foundation grants (Grant numbers PP00P1_183715 and 32003B_138413).

Conflict of interest

The authors declared that they had no conflict of interest with respect to their authorship or the publication of this article.

Acknowledgements

This study was conducted at the Brain and Behavior Laboratory (BBL) at the University of Geneva and benefited from the support of the BBL technical staff.

References

Atlas, L.Y., Bolger, N., Lindquist, M.A., Wager, T.D. (2010). Brain mediators of predictive cue effects on perceived pain. *The Journal of Neuroscience*, **30**, 12964–77.

Buhle, J., Wager, T.D. (2010). Performance-dependent inhibition of pain by an executive working memory task. *Pain*, **149**, 19–26.

Bushnell, M.C., Čeko, M., Low, L.A. (2013). Cognitive and emotional control of pain and its disruption in chronic pain. *Nature Reviews Neuroscience*, **14**, 502–11.

Duker, P.C., van den Bercken, J., Foekens, M.-A. (1999). Focusing versus distraction and the response to clinical electric shocks. *Journal of Behavior Therapy and Experimental Psychiatry*, **30**, 199–204.

Fan, L., Li, H., Zhuo, J., *et al.* (2016). The human Brainnetome atlas: a new brain atlas based on connectional architecture. *Cerebral Cortex*, **26**, 3508–26.

Friston, K.J., Worsley, K.J., Frackowiak, R.S.J., Mazziotta, J.C., Evans, A.C. (1993). Assessing the significance of focal activations using their spatial extent. *Human Brain Mapping*, **1**, 210–20.

Geuter, S., Boll, S., Eippert, F., Büchel, C. (2017). Functional dissociation of stimulus intensity encoding and predictive coding of pain in the insula. *eLife*, **6**, 1–22.

Hodes, R.L., Rowland, E.W., Lightfoot, N., Cleeland, C.S. (1990). The effects of distraction on responses to cold pressor pain. *Pain*, **41**, 109–14.

Hoegh, M., Seminowicz, D.A., Graven-Nielsen, T. (2019). Delayed effects of attention on pain sensitivity and conditioned pain modulation. *European Journal of Pain*, **23**, 1850–62.

Hung, Y., Gaillard, S.L., Yarmak, P., Arsalidou, M. (2018). Dissociations of cognitive inhibition, response inhibition, and emotional interference: voxelwise ALE meta-analyses of fMRI studies. *Human Brain Mapping*, **39**, 4065–82.

Keogh, E., Hatton, K., Ellery, D. (2000). Avoidance versus focused attention and the perception of pain: differential effects for men and women. *Pain*, **85**, 225–30.

Kragel, P.A., Kano, M., Oudenhove, L.V., *et al.* (2018). Generalizable representations of pain, cognitive control, and negative emotion in medial frontal cortex. *Nature Neuroscience*, **21**, 283–9.

Laird, A.R., McMillan, K.M., Lancaster, J.L., *et al.* (2005). A comparison of label-based review and ALE meta-analysis in the Stroop task. *Human Brain Mapping*, **25**, 6–21.

Legrain, V., Damme, S.V., Eccleston, C., Davis, K.D., Seminowicz, D.A., Crombez, G. (2009). A neurocognitive model of attention to pain: behavioral and neuroimaging evidence. *Pain*, **144**, 230–2.

McCaul, K.D., Monson, N., Maki, R.H. (1992). Does distraction reduce pain-produced distress among college students? *Health Psychology*, **11**, 210–7.

McLaren, D.G., Ries, M.L., Xu, G., Johnson, S.C. (2012). A generalized form of context-dependent psychophysiological interactions (gPPI): a comparison to standard approaches. *NeuroImage*, **61**, 1277–86.

Nouwen, A., Cloutier, C., Kappas, A., Warbrick, T., Sheffield, D. (2006). Effects of focusing and distraction on cold pressor-induced pain in chronic back pain patients and control subjects. *The Journal of Pain*, **7**, 62–71.

Petrovic, P., Petersson, K.M., Ghatan, P.H., Stone-Elander, S., Ingvar, M. (2000). Pain-related cerebral activation is altered by a distracting cognitive task. *Pain*, **85**, 19–30.

Posner, M.I., Petersen, S.E. (1990). The attention system of the human brain. *Annual Review of Neuroscience*, **13**, 25–42.

Riontino, L., Fournier, R., Lapteva, A., Silvestrini, N., Schwartz, S., Corradi-Dell'Acqua, C. (2022). Cognitive exertion affects the appraisal of one's own and other people's pain. *bioRxiv*.

Seminowicz, D.A., Davis, K.D. (2007a). A re-examination of pain–cognition interactions: implications for neuroimaging. *PAIN*, **130**, 8–13.

Seminowicz, D.A., Davis, K.D. (2007b). Interactions of pain intensity and cognitive load: the brain stays on task. *Cerebral Cortex*, **17**, 1412–22.

Seminowicz, D.A., Mikulis, D.J., Davis, K.D. (2004). Cognitive modulation of pain-related brain responses depends on behavioral strategy. *Pain*, **112**, 48–58.

Shackman, A.J., Salomons, T.V., Slagter, H.A., Fox, A.S., Winter, J.J., Davidson, R.J. (2011). The integration of negative affect, pain and cognitive control in the cingulate cortex. *Nature Reviews Neuroscience*, **12**, 154–67.

Sharvit, G., Corradi-Dell'Acqua, C., Vuilleumier, P. (2018). Modality-specific effects of aversive expectancy in the anterior insula and medial prefrontal cortex. *Pain*, **159**, 1529–42.

Sharvit, G., Lin, E., Vuilleumier, P., Corradi-Dell'Acqua, C. (2020). Does inappropriate behavior hurt or stink? The interplay between neural representations of somatic experiences and moral decisions. *Science Advances*, **6**, 1–14.

Silvestrini, N., Chen, J.-I., Piché, M., *et al.* (2020). Distinct fMRI patterns colocalized in the cingulate cortex underlie the after-effects of cognitive control on pain. *NeuroImage*, **217**, 116898.

Silvestrini, N., Corradi-Dell'Acqua, C. (2022). The impact of pain on subsequent effort and cognitive performance. *Journal of Psychophysiology*. Advance online publication.

Silvestrini, N., Rainville, P. (2013). After-effects of cognitive control on pain. *European Journal of Pain*, **17**, 1225–33.

Sprenger, C., Finsterbusch, J., Büchel, C. (2015). Spinal cord–midbrain functional connectivity is related to perceived pain intensity: a combined spino-cortical fMRI study. *Journal of Neuroscience*, **35**, 4248–57.

Tinnermann, A., Geuter, S., Sprenger, C., Finsterbusch, J., Büchel, C. (2017). Interactions between brain and spinal cord mediate value effects in nocebo hyperalgesia. *Science*, **358**, 105–8.

Tracey, I., Mantyh, P.W. (2007). The cerebral signature for pain perception and its modulation. *Neuron*, **55**, 377–91.

Tracey, I., Ploghaus, A., Gati, J.S., *et al.* (2002). Imaging attentional modulation of pain in the periaqueductal gray in humans. *Journal of Neuroscience*, **22**, 2748–52.

Valet, M., Sprenger, T., Boecker, H., *et al.* (2004). Distraction modulates connectivity of the cingulo-frontal cortex and the midbrain during pain—an fMRI analysis. *Pain*, **109**, 399–408.

Verstynen, T.D. (2014). The organization and dynamics of corticostriatal pathways link the medial orbitofrontal cortex to future behavioral responses. *Journal of Neurophysiology*, **112**, 2457–69.

Wager, T.D., Atlas, L.Y., Lindquist, M.A., Roy, M., Woo, C.-W., Kross, E. (2013). An fMRI-based neurologic signature of physical pain. *New England Journal of Medicine*, **368**, 1388–97.

Whitfield-Gabrieli, S., Nieto-Castanon, A. (2012). Conn: a functional connectivity toolbox for correlated and anticorrelated brain networks. *Brain Connectivity*, **2**, 125–41.

Wiech, K. (2016). Deconstructing the sensation of pain: the influence of cognitive processes on pain perception. *Science (New York, N.Y.)*, **354**, 584–7.

Woo, C.-W., Roy, M., Buhle, J.T., Wager, T.D. (2015). Distinct brain systems mediate the effects of nociceptive input and self-regulation on pain. *PLOS Biology*, **13**, e1002036.

Zalesky, A., Cocchi, L., Fornito, A., Murray, M.M., Bullmore, E. (2012). Connectivity differences in brain networks. *NeuroImage*, **60**, 1055–62.